Published April 5, 2010

First publ. in: The Journal of Cell Biology 189 (2010), 1, pp. 57-68
doi: 10.1083/jcb.200910074

JCB: Article

A dual function for chaperones SSB–RAC and the NAC nascent polypeptide–associated complex on ribosomes

Ansgar Koplin,[1] Steffen Preissler,[1,2] Yulia Ilina,[1] Miriam Koch,[1,2] Annika Scior,[1,2] Marc Erhardt,[1] and Elke Deuerling[1]

[1]Laboratory of Molecular Microbiology, Department of Biology, and [2]Konstanz Research School of Chemical Biology, University of Konstanz, 78457 Konstanz, Germany

The yeast Hsp70/40 system SSB–RAC (stress 70 B–ribosome-associated complex) binds to ribosomes and contacts nascent polypeptides to assist cotranslational folding. In this study, we demonstrate that nascent polypeptide–associated complex (NAC), another ribosome-tethered system, is functionally connected to SSB–RAC and the cytosolic Hsp70 network. Simultaneous deletions of genes encoding NAC and SSB caused conditional loss of cell viability under protein-folding stress conditions. Furthermore, NAC mutations revealed genetic interaction with a deletion of Sse1, a nucleotide exchange factor regulating the cytosolic Hsp70 network. Cells lacking SSB or Sse1 showed protein aggregation, which is enhanced by additional loss of NAC; however, these mutants differ in their potential client repertoire. Aggregation of ribosomal proteins and biogenesis factors accompanied by a pronounced deficiency in ribosomal particles and translating ribosomes only occurs in *ssbΔ* and *nacΔssbΔ* cells, suggesting that SSB and NAC control ribosome biogenesis. Thus, SSB–RAC and NAC assist protein folding and likewise have important functions for regulation of ribosome levels. These findings emphasize the concept that ribosome production is coordinated with the protein-folding capacity of ribosome-associated chaperones.

Introduction

The folding of newly synthesized proteins requires the assistance of a chaperone network. At the forefront of this network are ribosome-associated chaperones, which contact nascent polypeptides to control cotranslational protein folding and prevent aggregation or degradation of newly synthesized proteins (Bukau et al., 2000; Frydman, 2001; Hartl and Hayer-Hartl, 2002; Wegrzyn and Deuerling, 2005). Eukaryotic ribosomes are associated with both a Hsp70/40-based chaperone system and the nascent polypeptide–associated complex (NAC; Fig. 1 A). Both systems are abundant and conserved components of the eukaryotic cytosol, which dynamically bind to the large ribosomal subunit and interact with nascent polypeptides early during protein biogenesis (Pfund et al., 1998; Rospert et al., 2002; Hundley et al., 2005; Wegrzyn and Deuerling, 2005; Raue et al., 2007).

In yeast, the tripartite ribosome-bound Hsp70/40 system consists of the Hsp70 chaperone SSB (stress 70 B), which binds nascent chains, and ribosome-associated complex (RAC), a stable heterodimer formed by the Hsp70 homologue Ssz and the Hsp40 zuotin (Fig. 1 A). RAC acts as a cochaperone and stimulates ATP hydrolysis by SSB, thereby promoting substrate binding. Two functionally interchangeable SSB proteins (Ssb1 and Ssb2) exist in yeast, and the two protein sequences differ by only four amino acids (referred to as SSB hereafter). Yeast strains lacking either one or all three components of the chaperone triad show similar pleiotropic phenotypes, such as hypersensitivity to a wide range of cations, including translation-inhibiting cationic aminoglycosides and sensitivity to high salt concentrations and low temperatures (Pfund et al., 1998; Gautschi et al., 2002; Hundley et al., 2002; Kim and Craig, 2005).

Correspondence to Elke Deuerling: Elke.Deuerling@uni-konstanz.de

M. Erhardt's present address is Dept. of Biology, University of Utah, Salt Lake City, UT 84112.

Abbreviations used in this paper: NAC, nascent polypeptide–associated complex; NEF, nucleotide exchange factor; RAC, ribosome-associated complex; wt, wild type.

© 2010 Koplin et al. This article is distributed under the terms of an Attribution–Noncommercial–Share Alike–No Mirror Sites license for the first six months after the publication date (see http://www.rupress.org/terms). After six months it is available under a Creative Commons License (Attribution–Noncommercial–Share Alike 3.0 Unported license, as described at http://creativecommons.org/licenses/by-nc-sa/3.0/).

Supplemental Material can be found at:
http://jcb.rupress.org/content/suppl/2010/04/05/jcb.200910074.DC1.html

The Rockefeller University Press $30.00
J. Cell Biol. Vol. 189 No. 1 57–68
www.jcb.org/cgi/doi/10.1083/jcb.200910074

Konstanzer Online-Publikations-System (KOPS)
URL: http://nbn-resolving.de/urn:nbn:de:bsz:352-124939

THE JOURNAL OF CELL BIOLOGY

Downloaded from jcb.rupress.org on June 17, 2011

Published April 5, 2010

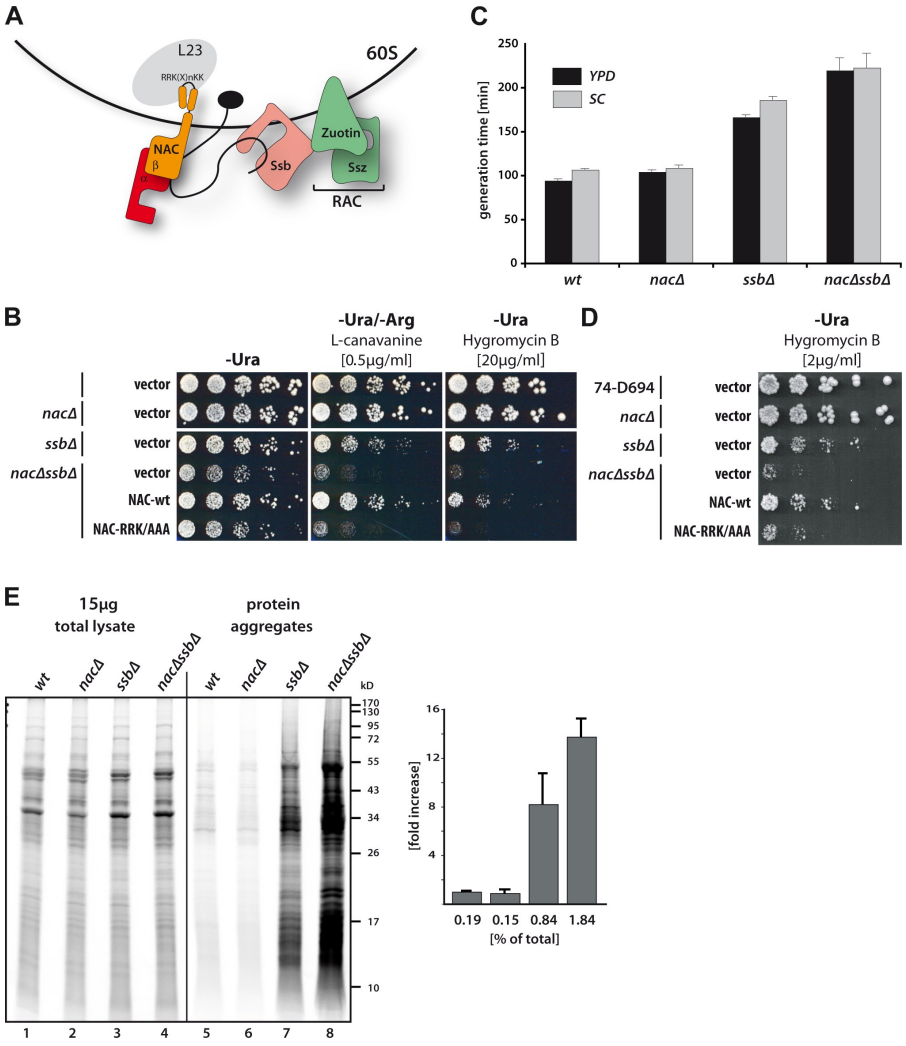

Figure 1. **The ribosome-associated factors NAC and SSB–RAC functionally cooperate on ribosomes.** (A) Schematic drawing of the ribosome-associated heterodimer NAC, which binds via a conserved motif (RRK-X_n-KK) to ribosomal protein L23 at the tunnel exit (black circle), and the tripartite chaperone system SSB–RAC. Emerging nascent polypeptides (black line) interact with NAC and/or SSB. (B) Growth analysis of wt and chaperone mutant cells. Serial dilutions of cells were spotted on synthetic complete media without uracil for plasmid selection and with drugs where indicated. Arginine was omitted when cells were plated on the arginine analogue L-canavanine. Cells were incubated for 3 d at 30°C. NAC-wt indicates cells expressing NAC from plasmid under its authentic promoter, whereas NAC-RRK/AAA indicates the expression of a NAC variant deficient in ribosome binding (Wegrzyn et al., 2006). (C) Generation time of wt and chaperone mutant cells in liquid culture grown in rich media (YPD) or synthetic complete media (SC) at 30°C. (D) Same as in B, but all mutations have been introduced into a different strain background (wt 74-D694). (E, left) Cells were pulsed for 1 min with [^{35}S]methionine, and after cell lysis, the aggregated protein material was isolated by sedimentation. 15 µg total lysate and isolated aggregated fractions were separated by SDS-PAGE for subsequent autoradiography. (right) Quantification of insoluble fractions in a percentage of total incorporated ^{35}S-label using ImageJ. Error bars indicate SD. Numbers below bars refer to one representative experiment.

NAC is a stable heterodimer composed of an α- and a β-NAC subunit (Fig. 1 A; Wiedmann et al., 1994; Reimann et al., 1999; Rospert et al., 2002). Although both subunits were shown to cross-link to nascent polypeptides (Wiedmann et al., 1994), only the β-NAC subunit contacts the ribosome via the conserved consensus motif RRK $(X)_n$ KK, located in its N terminus (Fig. 1 A). Mutations in this conserved NAC motif abolish ribosome binding and cross-linking to nascent polypeptides (Wegrzyn et al., 2006). Multiple potential functions for NAC have been proposed so far, including the control of protein translocation to the endoplasmic reticulum or into mitochondria. However, these functions of NAC remain a matter of debate because no consistent data could be obtained (Lauring et al., 1995; Powers and Walter, 1996; Möller et al., 1998; Raden and Gilmore, 1998; Wiedmann and Prehn, 1999). Additionally, given its ability to associate with ribosomes and nascent polypeptides, a chaperone-like function of NAC has been suggested (Bukau et al., 2000; Frydman, 2001; Hartl and Hayer-Hartl, 2002; Wegrzyn and Deuerling, 2005). However, yeast cells lacking NAC reveal no noticeable phenotype, and the in vivo function of NAC is still barely understood (Reimann et al., 1999).

In this study, we set out to investigate whether NAC is functionally interconnected to the chaperone network of the yeast cytosol. To this end, we combined knockout mutations in genes coding for NAC with SSB–RAC and characterized the phenotypes and subsequent consequences on protein folding. We found genetic and biochemical evidence that supports a function of NAC in the intricate chaperone network of the yeast cytosol. Moreover, we observed that NAC and SSB govern the abundance of ribosomal particles suggesting a new yet undiscovered function of these ribosome-associated chaperones in ribosomal biogenesis.

Results

Synergistic growth defects of cells simultaneously lacking NAC and SSB

To investigate whether both ribosome-associated systems NAC and SSB–RAC (Fig. 1 A) are functionally interconnected, we combined knockout mutations of all three genes coding for NAC subunits (*egd1Δ*, *btt1Δ*, and *egd2Δ*; referred to hereafter as *nacΔ*) with deletions of the two *SSB* genes (*ssb1Δ* and *ssb2Δ*; referred to hereafter as *ssbΔ*). Cells carrying the quintuple knockout mutations (*nacΔssbΔ* cells) were viable, however, they revealed a pronounced synthetic growth defect. At 30°C, *nacΔssbΔ* cells grew significantly slower than *nacΔ* or *ssbΔ* cells as judged

Downloaded from jcb.rupress.org on June 17, 2011

Published April 5, 2010

by the colony size on plates (Fig. 1 B) and an extended doubling time in liquid cultures (Fig. 1 C). Moreover, the application of low concentrations of drugs that impair protein synthesis or folding, such as the translation inhibitor hygromycin B or the arginine analogue L-canavanine, resulted in a severe decline in the viability of *nacΔssbΔ* cells. The plating efficiency was also decreased by several orders of magnitude as compared with control cells of wild type (wt), *nacΔ*, or *ssbΔ* (Fig. 1 B). As reported earlier, cells lacking only SSB revealed slower growth at 30°C in the presence or absence of drugs compared with wt cells, whereas cells lacking NAC showed no growth impairment (Fig. 1, B and C; Reimann et al., 1999; Kim and Craig, 2005).

Importantly, expression of wt NAC from a centromeric plasmid fully complemented the phenotype of *nacΔssbΔ* cells back to the character of the *ssbΔ* strain, whereas the expression of the NAC-RRK/AAA ribosome-binding mutant did not (Fig. 1 B). This implies that the observed phenotype is specific for NAC and critically depends on its ribosome association. The growth deficiency and the synergistic phenotype of cells lacking both NAC and SSB was reproducibly observed in another yeast background (Fig. 1 D) excluding clone- or strain-specific effects and suggesting general synthetic defects in the absence of these ribosome-associated proteins. Moreover, to confirm that the phenotype of *nacΔssbΔ* cells is related to SSB chaperone function in the triad, *nacΔ* mutations were combined with a *zuoΔ* mutation. This knockout combination resulted in similar synthetic defects as compared with *nacΔssbΔ* cells (Fig. S1 A). We also observed that cold sensitivity as well as salt sensitivity was more pronounced in cells lacking SSB and NAC, which is in contrast to cells lacking only SSB (unpublished data).

Thus, the synergistic growth defects of *nacΔssbΔ* cells reveal a genetic interaction between genes coding for NAC and SSB, suggesting that the two ribosome-associated systems in eukaryotes work in parallel or in partly overlapping pathways during de novo protein folding. The data support a function of NAC in protein biogenesis connected to the SSB–RAC chaperone system, and this function critically depends on the ribosome association of NAC.

Loss of NAC and SSB affects the folding of newly synthesized polypeptides

To investigate whether the folding of newly synthesized polypeptides is affected by the loss of the two ribosome-associated systems, log-phase cells lacking either one or both systems were pulsed for 1 min with [^{35}S]methionine in minimal media to label newly synthesized proteins. Subsequently, translation was stopped by the addition of cycloheximide, and aggregated proteins in these cells were isolated from cellular lysates by sedimentation analysis. The [^{35}S]methionine-labeling efficiency of the strains was similar, as judged by autoradiography of 15 µg total cell lysate (Fig. 1 E, lanes 1–4). Neither wt cells nor cells lacking NAC revealed a substantial amount of insoluble material, which is consistent with the lack of any observable *nacΔ* phenotype (Fig. 1 E, lanes 5 and 6). In contrast, the absence of SSB caused significant aggregation of a variety of newly made polypeptides. This aggregation tendency was more pronounced in cells lacking both SSB and NAC (Fig. 1 E, lanes 7 and 8). The aggregates included nascent (incomplete) polypeptides as well as proteins translated and released within the labeling period, thereby explaining the mixture of the radioactively labeled smear punctuated with discrete bands. Densitometric analysis of the aggregated ^{35}[S]-containing material showed that ~2% of newly synthesized proteins were aggregation prone in the absence of both NAC and SSB, whereas only about half the amount of newly made proteins became insoluble in cells lacking exclusively SSB (Fig. 1 E, bottom). Thus, cells lacking NAC and SSB show a synergistic defect in the folding of newly made proteins.

Ribosomal proteins and ribosomal biogenesis factors aggregate in cells lacking SSB and NAC

To identify the aggregation-prone species present in *nacΔssbΔ* cells, we prepared aggregates from logarithmically growing cells in quantitative amounts and separated the isolated insoluble fractions by SDS-PAGE for Coomassie staining (Fig. 2 A). In agreement with aforementioned results, pronounced protein aggregation was found in cells lacking SSB or both SSB and NAC, which mainly consisted of small-sized species with a molecular mass between 17 and 55 kD. The pattern of aggregated proteins in *ssbΔ* and *nacΔssbΔ* cells was very similar, albeit more pronounced in cells lacking both systems, suggesting that a similar set of client proteins are affected by the loss of SSB and NAC (Fig. 2 A). The major bands visible in the insoluble fraction prepared from *nacΔssbΔ* cells were excised from the Coomassie-stained gel and identified by mass spectrometry (Table I). A total of 64 proteins could be unambiguously identified, including predominantly ribosomal proteins (52 out of 64) from both ribosomal subunits and several ribosomal biogenesis factors involved in the biogenesis of the large and small subunit, such as Dbp8, Tif6, Nog1, and Rlp24, and the elongation factor EF-1a (Tef2). Western blot analysis with antibodies directed against ribosomal protein Rpl35 confirmed the aggregation of Rpl35 in *ssbΔ* cells, which was further enhanced in cells lacking SSB and NAC (Fig. 2 A, middle). Moreover, some cytosolic chaperones, including the Hsp40 homologues Ydj1 and Sis1, a subunit (Cct8) of the Cct chaperonin, and small heat shock protein Hsp26, were found in the pellet fraction, presumably because of cosedimentation with their unfolded substrates.

Different and not mutually exclusive scenarios could explain the aggregation of this set of proteins. Ribosomal proteins and ribosome biogenesis factors are perhaps particularly aggregation prone in cells lacking chaperones and thus aggregate upon synthesis before their engagement in ribosome assembly. Perhaps this also may render preribosomal particles aggregation prone because of incomplete maturation. Alternatively, nascent chains aggregate during translation and thereby pull ribosomes into the insoluble fraction. Because nascent chains are heterogenous, only the ribosomal proteins are visible as distinct bands in the Coomassie-stained gel.

To investigate whether ribosomal particles might be present in the aggregates, we tested for the presence of nucleic acids by ethidium bromide staining of aggregates. We detected

Downloaded from jcb.rupress.org on June 17, 2011

Published April 5, 2010

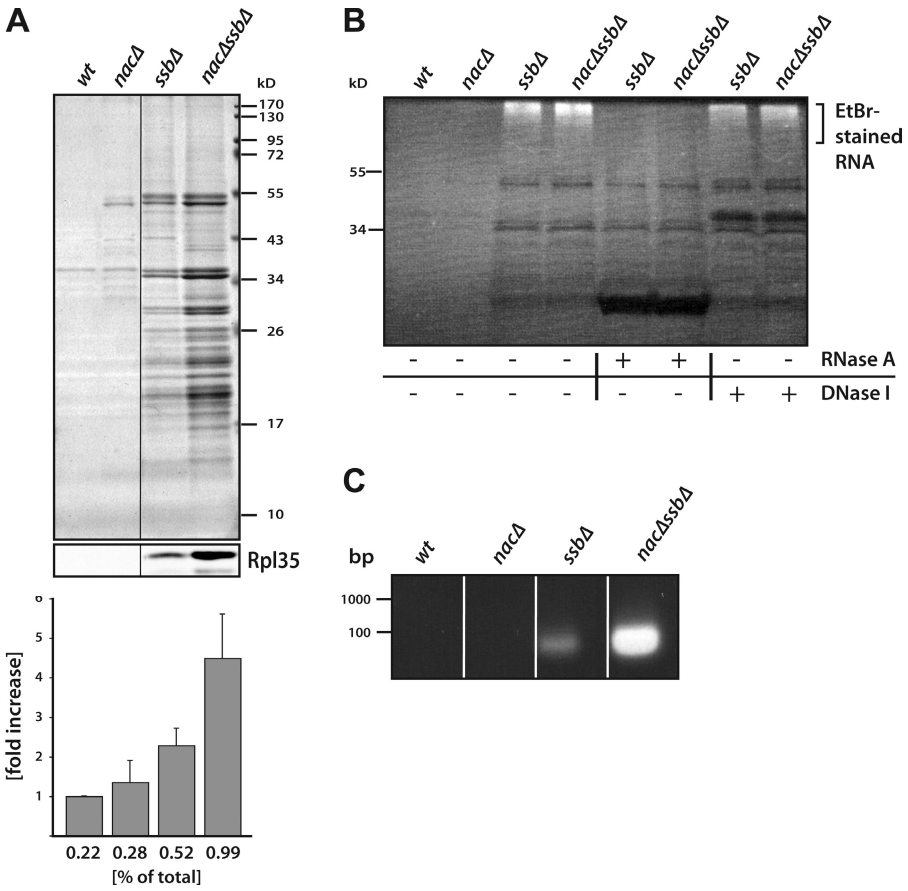

Figure 2. **Aggregation of ribosomal proteins and ribosomal biogenesis factors in cells lacking SSB and NAC.** (A) Quantitative preparation of aggregated material from wt and chaperone mutant cells under steady-state conditions. Cells were grown to logarithmic phase in YPD media at 30°C, and after lysis, aggregated material was isolated, separated by SDS-PAGE, and visualized by Coomassie staining. Black lines indicate that intervening lanes have been spliced out. (bottom) Western blotting revealed the aggregation of ribosomal Rpl35 and quantification of aggregated material (given in percentages of total protein) using ImageJ. Error bars indicate SD. (B) Isolated insoluble material was treated with RNaseA or DNaseI, separated via SDS-PAGE, and stained with ethidium bromide (EtBr). (C) Ethidium bromide–stained agarose gel showing the extracted RNA from aggregates isolated from wt and different mutant cells.

nucleic acid signals in aggregate samples isolated from *ssbΔ* and *nacΔssbΔ* cells (Fig. 2 B). Treatment with RNaseA completely abolished staining, whereas treatment with DNaseI did not, suggesting that RNA was present in the aggregate fractions derived from *ssbΔ* and *nacΔssbΔ* cells (Fig. 2 B). Isolation of RNA from the insoluble fractions identified small RNA fragments (<100 bp) specifically in *ssbΔ* and *nacΔssbΔ* samples (Fig. 2 C). The small size of the RNA fragments, which most likely resulted from shearing forces during the sonification steps of the aggregate preparation, did not permit Northern blot analyses to further characterize the RNA molecules. However, we applied the extracted RNA to a dot blot analysis using a digoxigenin-labeled DNA probe directed against unprocessed 35S and 27S rRNA and detected signals in the RNA samples extracted from *ssbΔ* and *nacΔssbΔ* aggregates (Fig. S2 A). These results suggest that ribosomal particles, including perhaps preribosomal species, are present in the insoluble fractions of *ssbΔ* and *nacΔssbΔ* cells. To exclude that ribosomal particles interact with aggregates and therefore sediment nonspecifically in our aggregation analysis, we mixed biotin-labeled ribosomes with lysates derived from wt or mutant cells prior to isolation of the insoluble material. Subsequently, the aggregate fractions were probed for the presence of biotin-tagged particles by Western blotting. No signals of biotin-labeled ribosomes were detected in the aggregate fractions, whereas biotin-labeled ribosomes could be quantitatively recovered by high speed centrifugation (Fig. S2, B–D). We conclude that ribosomal particles are specific components of the insoluble fractions isolated from cells lacking SSB and NAC, although we cannot estimate the quantitative contribution of ribosomal particles to the aggregated fractions.

Loss of SSB causes aggregation of ribosomal proteins and biogenesis factors

Ribosomal proteins and biogenesis factors are highly abundant proteins, which contain several complicated folds. We reasoned that if these proteins are especially prone to aggregation in SSB-deficient cells, their solubility may also be affected by the loss of other Hsp70s such as the cytosolic SSA proteins in yeast.

To test for this possibility, we investigated whether the deletion of Sse1, either alone or in combination with NAC, would cause aggregation of similar protein species. The yeast Hsp110 chaperone Sse1 functions as a nucleotide exchange factor (NEF) for multiple Hsp70s, including the two ribosome-associated SSBs and the four cytosolic Hsp70s, SSA1–4. Thus, deletion of Sse1 decreases the activity of the entire cytosolic Hsp70 network. It should be mentioned that although *sse1Δ* cells are viable as a result of overlapping functions of other NEFs, the deletion of all four *SSA* genes is lethal in yeast and thus cannot be directly investigated. Moreover, it is not known to what extent Sse1 affects the SSB and SSA systems.

Aggregation analysis revealed the accumulation of insoluble proteins in cells lacking Sse1 compared with wt or *nacΔ* cells. Additional deletion of NAC genes caused enhanced protein aggregation in Sse1-deficient cells similar to its effect in *ssbΔ* cells (Fig. 3 B). This finding further supports a role for NAC in the context of the Hsp70 chaperone network. The result

Downloaded from jcb.rupress.org on June 17, 2011

Published April 5, 2010

Table I. **Aggregated proteins isolated from *nacΔssbΔ* cells and identified by mass spectrometry**

Protein	Score
Ribosomal proteins 40S	
Rps1	7,657
Rps3	3,990
Rps4	4,296
Rps5	1,297
Rps6	11,431
Rps7	1,578
Rps8	6,429
Rps9	2,426
Rps10	1,264
Rps11	3,309
Rps13	5,559
Rps15	454
Rps16	1,141
Rps17	1,867
Rps18	2,452
Rps19	690
Rps20	1,522
Rps23	1,998
Rps24	9,741
Rps25	220
Rps26	1,218
Rps30	4,587
Ribosomal proteins 60S	
Rpl1	1,938
Rpl2	835
Rpl3	7,919
Rpl4	2,472
Rpl6	2,468
Rpl7	1,409
Rpl8	2,472
Rpl9	18,101
Rpl10	2,706
Rpl11	2,976
Rpl12	540
Rpl13	1,279
Rpl14	1,167
Rpl15	1,084
Rpl16	1,445
Rpl17	6,024
Rpl18	891
Rpl19	15,619
Rpl21	6,528
Rpl23	804
Rpl25	1,027
Rpl26	2,853
Rpl27	1,081
Rpl28	5,598
Rpl30	2,031
Rpl32	3,228
Rpl34	622
Rpl35	2,183
Rpl38	4,601
Rpl43	286
Ribosomal biogenesis factors	
Nog1	382
Dbp3	962
Dbp8	1,236
Tif6	535
Rlp24	241
Nip7	424
Nop58	1,507
Chaperones/translation factor	
Ydj1	1,858
Sis1	221
Hsp26	385
Cct8	809
Tef2	16,707

corresponded with an observed slow growth phenotype of *nacΔsse1Δ* cells compared with *sse1Δ* or *nacΔ* cells and the complementation of this growth defect by expression of the NEF Fes1 from a plasmid (Fig. 3 A). Strikingly, the pattern of aggregation-prone proteins isolated from *sse1Δ* and *nacΔsse1Δ* cells was clearly distinct from the aggregated species isolated from *nacΔssbΔ* (compare Fig. 2 A with Fig. 3 B), suggesting that SSB and SSA chaperones have a different client repertoire and the aggregates of *sse1Δ* cells represent a mixture of both. By mass spectrometry, we identified 13 proteins, which appeared as discrete bands in the aggregated fractions after SDS-PAGE. Three of them, Rpl3, Rps3, and Tef2, were prone to aggregate in both cells lacking SSB or Sse1 and, thus, may represent SSB substrates that are highly sensitive to a decreased SSB activity. In contrast, other proteins, including enzymes such as G6PDH (glucose-6-phosphate dehydrogenase) or pyruvate kinase, were only detected in cells lacking Sse1 and NAC and thus may represent substrates for the SSA system. Because the detected spectrum of aggregation-prone proteins in Sse1-deficient cells is unique compared with SSB-deficient cells, we conclude that the aggregation of ribosomal proteins and ribosomal biogenesis factors is highly specific for the loss of the ribosome-associated SSB system.

Loss of SSB and NAC functions leads to decreased levels of ribosomal subunits and translating ribosomes

We next examined whether the loss of SSB and NAC had any consequences on the level of ribosomes and translation. To this end, we compared the ribosomal profiles from wt cells with the profiles from cells lacking NAC and SSB. Total cell lysates were separated on a sucrose gradient using ultracentrifugation, and the resulting ribosomal profile characteristics of the gradient were measured at 254 nm. The peak heights as detected by $A_{254\,nm}$ could be used as sensitive indicators of the levels of each ribosomal species because equal absorption units of the samples were loaded. As evident from the ribosomal profile (Fig. 4 A), the absence of SSB and, more significantly, the simultaneous loss of SSB and NAC had severe consequences on the ribosomal species found in the cytosol of these cells. We detected a strong reduction of the 80S and polysome peaks in *ssbΔ* cells,

Downloaded from jcb.rupress.org on June 17, 2011

Published April 5, 2010

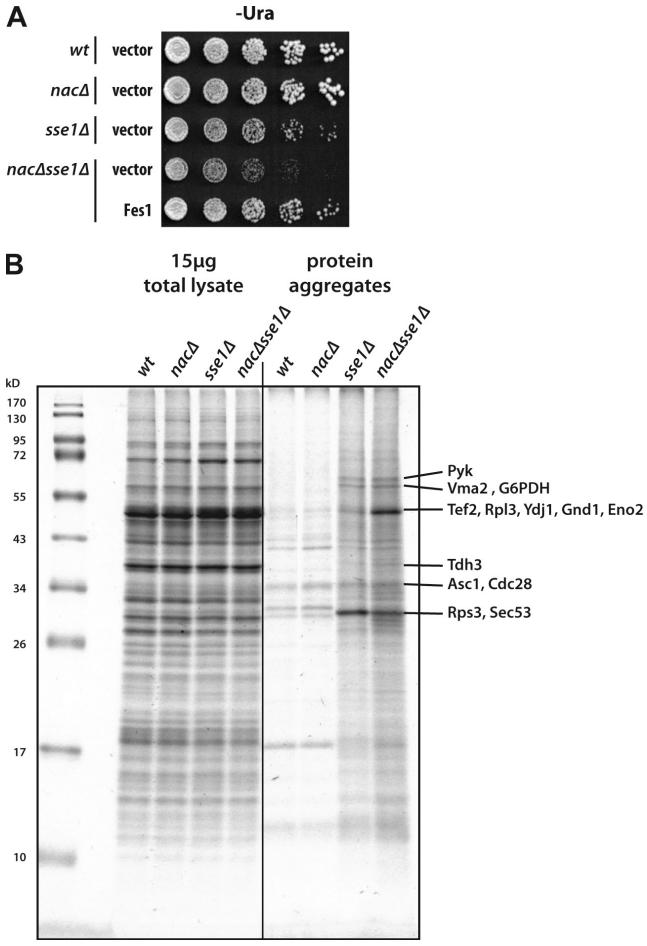

Figure 3. **Analysis of growth and protein aggregation in cells lacking Sse1 and NAC.** (A) Serial dilutions of wt and mutant cells were spotted on plates containing synthetic medium without Uracil for plasmid selection. Cells either carried the empty vector (control) or were transformed with a 2 µ vector encoding Fes1 as indicated. (B) Quantitative preparation of aggregated material from wt and chaperone mutant cells. Cells were grown to logarithmic phase in YPD media at 30°C, and after lysis, aggregated material was isolated, separated by SDS-PAGE, and visualized by Coomassie staining. 15 µg protein of total lysate (left) and isolated aggregated proteins (right) were loaded. Aggregated proteins identified by mass spectrometry analysis are indicated.

which was even more pronounced in *nacΔssbΔ* cells, indicating that cells lacking SSB and NAC have a reduced translational activity (Fig. 4 A). Quantification of integrated peak areas of the ribosome profiles confirmed a severe decrease in the total ribosome level, including the reduction of the polysome moieties in cells lacking SSB and NAC (Fig. 4 C). Moreover, in *ssbΔ* cells, and more distinctly in *nacΔssbΔ* cells, the formation of ribosomal half-mers was visible by a shoulder in the 80S and polysome peaks (Fig. 4 A, arrows). Ribosomal half-mers represent ribosomal species with an uncomplexed 40S portion. Such species are frequently observed in cells with defects in ribosome biogenesis, causing an impaired balance of 60S and 40S ribosomal subunits (Basu et al., 2001; Sydorskyy et al., 2003). We also investigated the ribosomal profiles of *sse1Δ* and *nacΔsse1Δ* cells and found reduced polysome peaks; however, this effect was less apparent compared with *ssbΔ* and *nacΔssbΔ* cells because deletion of *SSE1* causes only partial deprivation of SSB function (Fig. S3).

Next, we treated the lysate with EDTA before loading on sucrose gradients to dissociate 80S and polysomes into their subunits, which allowed us to monitor the total levels of 40S and 60S subunits in mutant and wt cells (Fig. 4 B). As evident by the changes in the peak heights, cells lacking SSB revealed a pronounced decrease in both 40S and 60S subunit levels. Again, the additional loss of NAC considerably aggravated this defect, whereas loss of NAC alone had only little impact on the levels of ribosomal subunits. Quantification of the total amount of 60S particles in wt and mutant cells by Western blotting with antibodies directed against the large ribosomal protein Rpl25 confirmed that the total amount of 60S particles was decreased by >50% in *nacΔssbΔ* cells compared with wt (Fig. 4 D). To test whether an enhanced turnover of ribosomal proteins may contribute to the deficit of 60S particles, we performed a cycloheximide inhibition experiment of exponentially growing wt and mutant cells and analyzed the decay of Rpl25. Although the total level of Rpl25 was lower in *nacΔssbΔ* cells compared with wt, no enhanced decay of this ribosomal protein was detected (Fig. 4 E). Therefore, we assume that SSB and NAC do not affect the turnover of ribosomal proteins but rather modulate production and assembly of ribosomal components. Furthermore, we conclude that the loss of SSB and NAC reduces the levels of ribosomal particles and consequently the amount of actively translating ribosomes.

SSB and NAC control ribosome biogenesis

To investigate a potential role of SSB and NAC in ribosome biogenesis more closely, we introduced a plasmid in wt and mutant cells expressing GFP-tagged ribosomal protein Rpl25. (Fig. 5 A). In wt and *nacΔ* cells, GFP-L25 was incorporated into mature ribosomes, and therefore, the majority of the fluorescence signal was found in the cytoplasm. Only very few wt (2%) and *nacΔ* (5%) cells revealed a nuclear staining, which is in agreement with earlier data (Hurt et al., 1999). In contrast, *ssbΔ* and *nacΔssbΔ* mutant cells showed strong nuclear accumulation of L25-GFP in ∼19% and 28% of GFP-positive cells, respectively. This result suggests a defect in L25 incorporation into mature 60S ribosomal particles in *ssbΔ* and even more distinct in *nacΔssbΔ* cells and emphasizes a role of SSB and NAC in ribosome production. Interestingly, we observed punctate Rpl25-GFP signals in the DAPI-stained area of the nucleus for *ssbΔ* and *nacΔssbΔ* cells compared with wt, which might reflect aggregates in or close to the nucleus (Fig. 5 A).

Recently, another yeast ribosome-associated chaperone, the Hsp40 Jjj1, was shown to be specifically involved in ribosome biogenesis but not in protein folding. Jjj1 acts on the release of shuttling biogenesis factors from the pre-60S particle in the cytosol, thereby promoting maturation of 60S subunits and allowing efficient nucleocytoplasmic recycling of biogenesis factors (Demoinet et al., 2007; Meyer et al., 2007). This prompted us to test for the combined deletions of the *JJJ1* gene with *SSB1* and *SSB2* genes (*ssbΔ*), but initial attempts to generate this triple knockout failed. Therefore, we first introduced a *URA3*-based plasmid expressing Ssb1 in *ssbΔ* cells and subsequently introduced the genomic *JJJ1* deletion. *SsbΔjjj1Δ* cells expressing Ssb1 from a plasmid under its authentic promoter

Downloaded from jcb.rupress.org on June 17, 2011

Published April 5, 2010

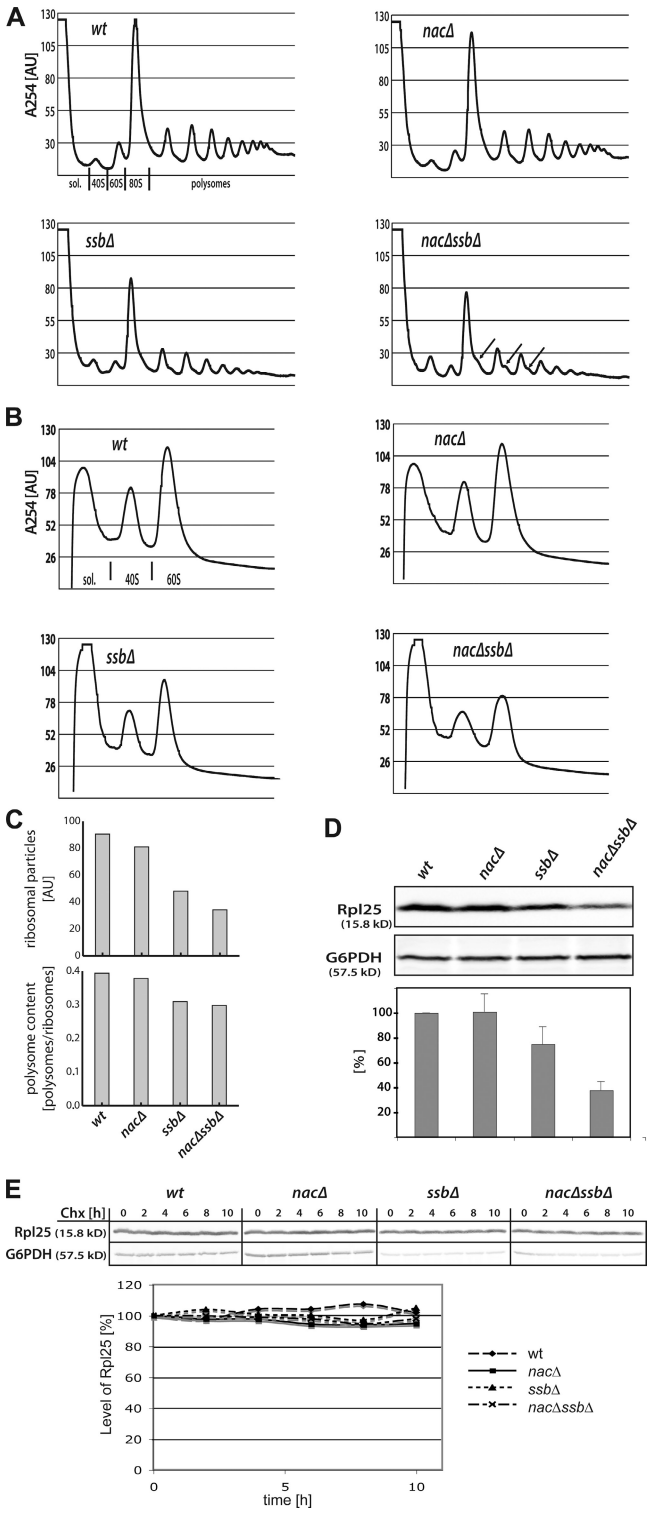

Figure 4. **Ribosomal profiles reveal a stoichiometric imbalance in 60S to 40S subunit ratio and the formation of half-mer ribosomes in cells lacking SSB and NAC.** (A) Lysates of indicated wt and mutant yeast cells were prepared, and eight A_{260} units were loaded on 15–45% linear sucrose gradients to fractionate cytosolic and ribosomal particles after centrifugation by readout at A_{254}. The distribution of cytosolic (sol.) and diverse ribosomal fractions in the gradient is indicated below the profile of the wt. Arrows in the profiles of *nacΔssbΔ* cells indicate the shoulder in the 80S and polysomal peaks as a result of the formation of ribosomal half-mers. Profiles are representative for three independent runs. (B) Profiles of dissociated ribosomes showing 40S and 60S ribosomal subunits. (C) Quantification of the peak areas of ribosomal profiles shown in A (top) using the program Fityk, and the portion of polysomes in total ribosomal particles given as the ratio of polysomes versus total ribosomes (bottom). (D) Loss of SSB and NAC reduces the level of 60S ribosomal particles. Quantification of 60S ribosomal particles by Western blot analysis of ribosomal protein Rpl25 using similar OD_{600} of cells for subsequent immunodetection (top) and quantification of Rpl25 protein (bottom). Wt level was set to 100%. Western blotting against cytosolic G6PDH served as loading control. Error bars indicate SD. (E) Decay of 60S ribosomal particles after cycloheximide (Chx) treatment was followed over 10 h by Western blotting against the 60S ribosomal protein Rpl25 (top), and quantification is shown (bottom). G6PDH served as loading control.

were viable at 30°C on selective media, which is comparable with cells lacking only SSB or Jjj1 (Fig. 5 B). In contrast, loss of the Ssb1-encoding plasmid by 5-FOA treatment caused synthetic lethality of cells deleted for both SSB and Jjj1, whereas cells lacking individual chaperones remained viable after the plasmid loss. We conclude from these data that SSB and Jjj1 work in distinct pathways during the production of ribosomes, and the combined loss of both activities causes cell death as a result of the destructive impairment in ribosome biogenesis.

Discussion

Our results provide the first in vivo evidence that NAC is functionally connected to the Hsp70 chaperone network. NAC genetically interacts and functionally collaborates with SSB–RAC and Sse1 in the folding of newly synthesized proteins. Moreover, we discovered a second and novel function of SSB–RAC and NAC in regulating the abundance of ribosomal particles, suggesting an important role for these ribosome-associated systems in the biogenesis of ribosomes.

The finding that NAC associates with ribosomes and interacts with the nascent chain previously evoked the hypothesis that this complex might be involved in cotranslational folding processes (Bukau et al., 2000; Frydman, 2001; Hartl and Hayer-Hartl, 2002). However, this assumption was contentious for quite some time because of the lack of any in vivo phenotype correlated with protein folding or chaperone networks. In this study, we now provide in vivo evidence that NAC is functionally connected to the chaperone network that assists the folding of newly synthesized proteins in the eukaryotic cytosol. Deletion of NAC alone has no detectable consequences for the growth of yeast cells or the de novo folding of newly synthesized proteins. In contrast, deletion of NAC in the absence of the Hsp70 chaperone SSB or any other member of this Hsp70/40 chaperone system impaired growth at 30°C and resulted in a severe drop of cell viability on plates containing hygromycin B or L-canavanine. Additionally, the double mutant showed enhanced aggregation of newly synthesized proteins (Fig. 1 E). Thus, the phenotype of NAC becomes apparent only in absence of SSB–RAC, suggesting that NAC and the Hsp70/40 system work in overlapping or parallel pathways during protein folding and are able to functionally collaborate with each other. The fact that only ribosome-associated NAC can complement the phenotype, but not a NAC mutant deficient in ribosomal attachment, demonstrates that NAC cooperates with SSB–RAC exclusively on ribosomes (Fig. 1, B and D). In the absence of NAC, the

Downloaded from jcb.rupress.org on June 17, 2011

Published April 5, 2010

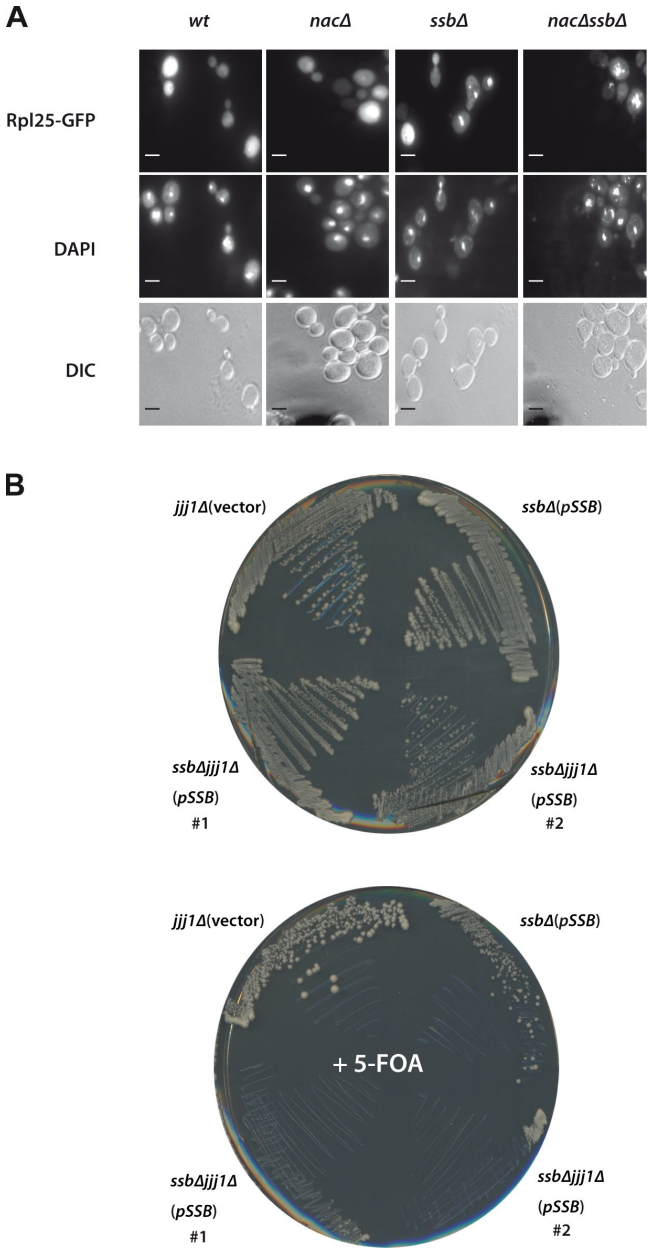

Figure 5. **Involvement of SSB and NAC in ribosomal biogenesis.** (A, top) Expression of Rpl25-GFP in wt and mutant cells. *NacΔ and nacΔssbΔ* deletion strains show accumulation of the nuclear Rpl25-GFP signal. (bottom) The localization of Rpl25-GFP signal in cells was visualized by fluorescence and differential interference contrast (DIC) microscopy. (middle) DAPI was used to visualize nuclei. Bars, 2 µm. (B) SSB genetically interacts with Jjj1. The triple *ssb1Δ ssb2Δ jjj1Δ* mutants (clone #1; #2) carrying the wt versions of the *SSB1* gene on a *URA3*-based plasmid were streaked on SC-URA and 5-FOA plates and incubated for 5 d at 30°C. The *ssbΔ* mutant carrying *SSB1* wt gene on the plasmid and *jjj1Δ* mutant containing empty vector served as controls.

function of SSB–RAC is sufficient to serve as a potent backup system. The finding that NAC contributes to the chaperone network was further emphasized by the genetic interaction suggested by the deletions of genes coding for NAC and Sse1, an NEF regulating both the SSB and SSA types of Hsp70s in the yeast cytosol.

How may NAC contribute to the folding of newly synthesized proteins? According to independent cross-linking studies, it is known that NAC acts very early on nascent polypeptides with a length of ∼17 amino acids in vitro, whereas SSB cross-links to nascent chains of a length of ∼58 amino acids, suggesting that NAC may act first, albeit comparative cross-linking studies have not been performed yet (Wang et al., 1995; Pfund et al., 2001). Moreover, it has been demonstrated that NAC protects nascent chains against proteolytic attack (Wang et al., 1995). Such a protective function as described for NAC may promote the efficient interaction of newly synthesized proteins with the ribosome-associated SSB–RAC chaperone system as well as with downstream-acting chaperones of the SSA type. Whether NAC itself displays a canonical chaperoning function with the capacity to prevent aggregation and to promote folding of unfolded proteins awaits further detailed biochemical analysis.

The most intriguing new finding of this study is that the loss of ribosome-associated chaperones SSB and NAC strongly affected the levels of ribosomal subunits and translating ribosomes, which is likely the result of a defect in ribosome biogenesis. Deletion of SSB alone already caused a pronounced reduction of ribosomal particles; however, this defect was enhanced in the absence of NAC, suggesting a collaborative action of both chaperones for this function as well. A role of SSB and NAC in ribosome biogenesis is supported by several different lines of evidence: (a) ribosomal proteins together with some ribosomal biogenesis factors and RNA are major constituents of the aggregates isolated from *nacΔssbΔ* cells, (b) ribosomal profiling and Western blot analysis revealed significantly decreased levels of 60S and 40S subunits, the formation of ribosomal halfmers, and a severe drop in actively translating 80S moiety and polysomes. Moreover, (c) cells lacking SSB and NAC accumulate ribosomal L25-GFP in the nucleus, and finally, (d) the combined deletion of SSB and Jjj1, which is described to have an active role in late steps of ribosome biogenesis of the 60S subunit, caused cell death (Demoinet et al., 2007; Meyer et al., 2007). Interestingly, recent work by Sahi and Craig (2007) showed that overexpression of Jjj1 can in part complement the phenotype of a *zuoΔ* deletion strain. They also showed that Hsp40 Jjj1 does stimulate the ATPase activity of SSA but not of SSB, which suggests that the Jjj1–SSA and SSB–RAC chaperone systems operate as defined chaperone systems in ribosomal biogenesis.

What might be the mechanistic basis for the role of SSB and NAC in ribosome biogenesis? Different models are plausible, which are not mutually exclusive. Our finding that ribosomal biogenesis factors and ribosomal proteins, which are required for the biogenesis of the small and large subunits, are constituents of the aggregates that accumulate in *nacΔssbΔ* cells suggests that these ribosome biogenesis factors and proteins are among the major clients of SSB and NAC (Fig. 6). SSB and NAC may bind to ribosomal client proteins immediately upon their synthesis to prevent misfolding and perhaps even accompany these aggregation-prone proteins until they are engaged in ribosome assembly. Loss of SSB and NAC hampers de novo folding and activity of ribosomal proteins and biogenesis factors, thereby leading to a deficiency in the production of ribosomal particles (Fig. 6). Thus, the function of SSB and NAC

Downloaded from jcb.rupress.org on June 17, 2011

Published April 5, 2010

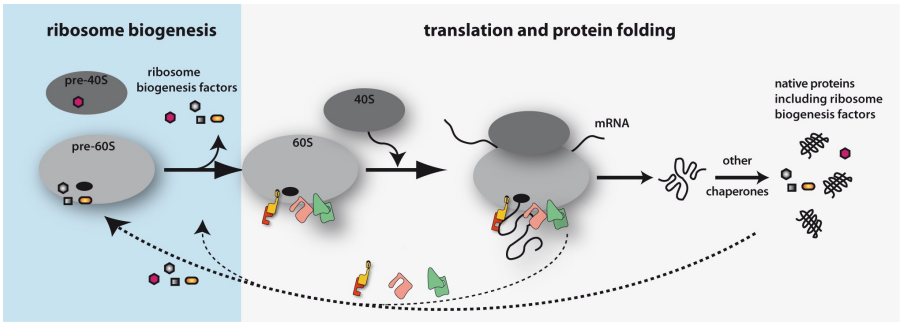

Figure 6. **Model indicating that NAC and SSB–RAC link chaperone-assisted de novo protein folding with the production of ribosomes.** NAC (yellow/red) and SSB–RAC (pink/green) associate with ribosomes and contact nascent polypeptides during synthesis to assist de novo protein folding. Some ribosome biogenesis factors and ribosomal proteins are among the potential client proteins, which particularly rely on NAC and SSB to fold into their active conformations and to support the assembly of ribosomal subunits. Moreover, NAC and SSB–RAC bind to ribosomes in a dynamic manner and may also directly contribute to the maturation of ribosomal subunits during ribosome biogenesis. The dual function of NAC and SSB–RAC in ribosome production and chaperone-assisted protein folding aligns ribosome production and protein synthesis with the folding capacity of ribosome-associated chaperones.

in chaperoning nascent chains of ribosomal proteins and biogenesis factors would directly translate into consequences for ribosome biogenesis. Such a scenario would explain all defects observed in *nacΔssbΔ* cells, including the finding that the level of both subunits is decreased in these chaperone-deficient cells. Interestingly, a recent study suggests that the N-terminal ubiquitin moiety of the ribosomal protein Rps31 serves a role as chaperone to facilitate the correct folding and assembly of Rps31 into 40S particles (Lacombe et al., 2009). Besides Rps31, another ribosomal protein, Rpl40, is fused to a ubiquitin moiety in yeast. Remarkably, both proteins were not found among the major aggregation-prone species identified in the aggregation analysis of *nacΔssbΔ* cells. Moreover, a very similar finding was recently described for the ribosome-associated chaperone trigger factor in bacteria. Trigger factor was suggested to bind to newly synthesized ribosomal proteins and thereby to facilitate the biogenesis of ribosomal complexes (Martinez-Hackert and Hendrickson, 2009).

Another possibility is that SSB–RAC and NAC display prime functions in ribosome biogenesis distinct from their chaperone function for nascent polypeptides. It is assumed that SSB–RAC and NAC bind transiently to ribosomes and cycle on and off the translation machinery (Fig. 6). This would allow them to serve other functions in the cell as well, e.g., promoting a distinct step of ribosome assembly before the particles are activated for translation. Interestingly, the aggregates isolated from cells lacking SSB and NAC contain several nuclear ribosome biogenesis factors (e.g., Dbp3, Dbp8, and Nog1) and perhaps premature nuclear 35S and/or 27S rRNA, which indicates that some of the aggregates originate from the nucleus. This finding, together with the observation that Rpl25-GFP accumulates in the nucleus of *nacΔssbΔ*, suggests that the loss of SSB and NAC causes defects already during early steps of ribosome biogenesis in the nucleolus. Indeed, a study in this issue by Albanèse et al. provides evidence for a role of SSB–RAC in assisting ribosome biogenesis in the nucleus.

Finally, SSB and NAC might contribute to the regulation of ribosomal particles at the transcriptional level. During preparation of this manuscript, von Plehwe et al. (2009) reported about the involvement of SSB in glucose signaling via the SNF1 kinase network. The authors suggested that SSB, by an unknown mechanism, keeps SNF1 kinase in a dephosphorylated state in the presence of high glucose levels. Because phosphorylated SNF1 kinase negatively regulates transcription of ribosomal components, the loss of SSB may cause enhanced SNF1 phosphorylation, thereby reducing ribosome production indirectly at the transcriptional level. However, we found no difference in SNF1 phosphorylation in *ssbΔ* and *nacΔssbΔ* cells compared with wt cells, and all strains responded similarly well to low glucose levels leading to enhanced SNF1 phosphorylation (Fig. S1 B). Thus, the global defect in ribosome biogenesis in cells lacking SSB and NAC detected in this study is not primarily caused by a dysfunction of SNF1 dephosphorylation under the growth conditions used in our analysis. It may well be that the different yeast strain backgrounds used by von Plehwe et al. (2009) and in our study may account for the variations in SNF1 signaling.

Cells lacking both ribosome-associated systems are viable under normal growth conditions but show slow growth accompanied by misfolding and aggregation of ~2% of newly synthesized protein. However, very low concentrations of drugs that interfere with protein synthesis or folding caused lethality in cells lacking SSB and NAC, emphasizing the profound impact of these ribosome-associated chaperones on cell physiology and cell viability.

Interestingly, the loss of SSB and NAC did not provoke the induction of a heat shock response at permissive temperature (Fig. S1 B). Loss of SSB and NAC does, however, cause a severe decrease in the amount of ribosomal particles and, consequently, a decrease in the level of translating ribosomes. Ribosome production is one of the most energy-consuming processes in cells and is assumed to be tightly regulated by multiple environmental and physiological cues. This study describes a new cellular link between ribosome production and the function of ribosome-associated chaperone systems (Fig. 6). This link puts forward the attractive concept that the level of ribosome production for protein synthesis can be matched with the protein-folding capacity of ribosome-associated chaperones. We speculate that the adjusted level of actively translating ribosomes in cells lacking SSB and NAC may allow cells to cope

Downloaded from jcb.rupress.org on June 17, 2011

Published April 5, 2010

with the loss of chaperone function and thereby reestablish protein homeostasis unless additional stress is applied (e.g., by drugs interfering with protein folding). How SSB and NAC may act as sensors for the folding capacity of the cell and how they probe ribosome production accordingly awaits further analysis.

Materials and methods

Strains, plasmids, and growth conditions

wt and single knockout cells were obtained from BY series of the EUROSCARF strain collection (Brachmann et al., 1998) or derivatives of the strain 74-D694 (Table S1; Bailleul et al., 1999). Additional gene disruptions in these backgrounds were generated by direct replacement of the appropriate coding regions with the *His3MX6* cassette (Longtine et al., 1998), the *NatMX4* cassette (Goldstein and McCusker, 1999), and the *ble* and *LEU2* cassette (Güldener et al., 2004). The correct insertion of the marker cassettes was confirmed by PCR from genomic DNA and by Western analysis with antibodies directed against the proteins encoded by the genes targeted by mutagenesis. Standard yeast protocols were used for transformations (Guthrie and Fink, 2004). The *sse1Δ* strain is from BY series of the EUROSCARF (*MATa*, *his3*, *leu2*, *met15*, *ura3*, and *sse1::kanMX4*), and *nacΔsse1Δ* (*MATa; met15; ura3; sse1::kanMX4; egd1::HIS3; egd2::LEU2; btt1::ble*) is a derivative thereof.

NAC-wt and NAC-RRK/AAA-encoding plasmids were generated by cloning a PCR-amplified EGD2 (derived from yeast genomic DNA, including endogenous promoter and terminator regions) into pRS316-EGD1-wt and pRS316-EGD1-RRK/AAA, respectively (Wegrzyn et al., 2006).

For the generation of the *ssb1Δ ssb2Δ jjj1Δ* triple-deletion strain, *JJJ1* was knocked out by the LEU2 cassette carrying the flanking regions of the *JJJ1* gene in the *ssb1Δ ssb2Δ* deletion strain containing the plasmid (p*SSB*) expressing wt *SSB1*. Mutant cells were checked by PCR, and two positive clones (#1 and #2) were streaked on SC-URA and 5-FOA plates (final concentration of 5-FOA was 1 mg/ml) to select for loss of the URA3 cassette. Additionally, the plasmid with URA3 marker containing *SSB1*, wt versions, and empty vector was transformed into the *ssb1Δ ssb2Δ* double mutant and the *jjj1Δ* single-deletion strain and transformants were streaked on SC-URA and 5-FOA plates.

The plasmid used for GFP experiments was made by PCR fusion of the GFP via a linker (GASG) to the C-terminal end of the genomic *RPL25* fragment and ligated into the vector backbone (pRS426). The *RPL25* gene of the resulting plasmid (Rpl25-GFP) was expressed from its native promoter.

Unless otherwise indicated, yeast cells were grown at 30°C in YPD (1% yeast extract, 2% peptone, and 2% dextrose) or defined synthetic complete (SC) media (6.7 g/liter YNB, 0.79 g/liter CSM mix, and 2% dextrose). Analysis of cell growth was performed at least three times.

Isolation of aggregated proteins and identification by mass spectrometry

50 OD_{600} units of logarithmically growing cells in YPD medium were harvested, and cell pellets were frozen in liquid N_2. For preparation of cell lysates, the pellets were resuspended in lysis buffer (20 mM Na-phosphate, pH 6.8, 10 mM DTT, 1 mM EDTA, 0.1% Tween, 1 mM PMSF, protease inhibitor cocktail [Roche], 3 mg/ml zymolyase T20, and 1.25 U/ml benzonase) and incubated at room temperature for 20 min. Chilled samples were treated by tip sonication (Branson; eight times at level 4 and duty cycle 50%) and centrifuged for 20 min at 200 *g* at 4°C. Supernatants were adjusted to identical protein concentrations, and aggregated proteins were pelleted at 16,000 *g* for 20 min at 4°C. After removing supernatants, aggregated proteins were washed twice with 2% NP-40 (in 20 mM Na-phosphate, pH 6.8, 1 mM PMSF, and protease inhibitor cocktail), sonicated (six times at level 4 and duty cycle 50%), and centrifuged at 16,000 *g* for 20 min at 4°C. Aggregated proteins were washed in NP-40–deficient buffer (sonication, four times at level 2 and duty cycle 65%), boiled in SDS sample buffer, separated by SDS-PAGE (14%), and analyzed by Coomassie staining. Experiments were performed at least three times with similar results. Identification of isolated aggregates by mass spectrometry was performed according to previously described protocols (Kramer et al., 2002; Wegrzyn et al., 2006). For significant protein identification, a score threshold of 200 was chosen.

For radioactive labeling of newly synthesized proteins, cells were starved for 1 h in methionine-free SC medium. The cells were labeled with 20 µCi/ml [^{35}S]methionine for 1 min, chilled quickly, and treated with 300 µg/ml cycloheximide to stop protein translation. ^{35}S-labeled aggregates were isolated, separated via SDS-PAGE, and visualized by autoradiography in FLA-9000 (Fujifilm).

Preparation of yeast extracts and ribosomal profiling

Yeast cells were grown at 30°C in YPD media to an OD_{600} of 0.8–1, rapidly chilled on ice, and harvested in the presence of 100 µg/ml cycloheximide to stabilize translating ribosomes. Preparation of cell extract was performed by glass bead disruption in lysis buffer (25 mM Tris-HCl, pH 7.5, 40 mM KCl, 7.5 mM $MgCl_2$, 100 µg/ml cycloheximide, 1 mM DTT, 1 mM PMSF, and protease inhibitor cocktail). After disruption of the cells, Triton X-100 and sodium deoxycholate were added to a final volume of 0.25% each. Eight units of A_{260nm} of each lysate were loaded onto an 11 ml 15–45% linear sucrose gradient prepared in lysis buffer (Gradient Master; Biocomp Instruments) and centrifuged for 2 h at 39,000 rpm in a rotor (TH-641; Sorvall) at 4°C. Gradients were fractionated from top to bottom with a density gradient fractionator (Teledyne Isco, Inc.), and A_{254} was monitored to detect cytosolic fraction, ribosomal subunits, monosomes, and polysomes. Data were recorded and processed with PeakTrak V1.1 (Teledyne Isco, Inc.). Experiments were performed at least three times with similar results.

Antibodies, Western blot analysis, and quantification

Rabbit polyclonal antibodies were raised against purified Ssa1p, Ssb1p, Zuo1p, and the NAC complex. Production of antibodies against ribosomal yeast Rpl25 (L25 corresponding to L23 in bacteria) and yeast Rpl35 (L35, corresponding to L25 in bacteria) were described previously (Kramer et al., 2002; Rauch et al., 2005). Hsp104 antibody was provided by B. Bukau, and antiserum recognizing G6PDH was obtained from Sigma-Aldrich. Protein samples separated via SDS-PAGE were transferred and immobilized onto nitrocellulose membrane (GE Healthcare). For detection, different dilutions of primary antibodies were applied (anti-SSA, 1:50,000; anti-Hsp104, 1:20,000; anti-SSB, -Zuo, -NAC, -L35, and -G6PDH, 1:10,000; and anti-L25, 1:5,000). For detection of primary antibodies, fluorescence-labeled secondary antibodies (DY-682; Dyomics) were applied and visualized with the FLA-9000 system (Fujifilm). Densitometric analysis of pixel intensities was performed using ImageJ (National Institutes of Health). Experiments were performed at least three times.

Microscopy

The plasmid Rpl25-GFP was transformed into the desired strain backgrounds, and the transformants were grown in SC-URA medium until OD_{600} was ~0.3–0.5. For DNA staining, DAPI was added to the cell suspension at a final concentration of 100 µg/ml. Cells were visualized on a microscope (37081 Visitron Systems; Carl Zeiss, Inc.) fitted with a 100× Plan Apochromat oil objective, and fluorescence was observed using standard FITC and DAPI filter sets at room temperature and PBS, pH 7.4, as imaging medium. For each strain, at least 200 GFP-positive cells were analyzed for cytoplasmic or nuclear accumulation of L25-GFP. Pictures were taken with Spot Pursuit (model 23.0), and 1.4 MP Monochrome without irradiation and Visitron Systems were used as acquisition software.

Cycloheximide decay analysis

Cells were grown at 30°C to logarithmic phase in YPD medium. 200 µg/ml cycloheximide was added to stop protein synthesis, and cells were harvested at the indicated time points. Cell extracts derived from similar cell numbers were prepared by standard alkaline lysis and subjected to SDS-PAGE and Western blotting.

RNA extraction from aggregates and dot blot analysis

Aggregates from the different yeast mutants were used to isolate RNA according to the protocol described previously (Chomczynski and Sacchi, 1987). For dot blot analysis, 3 µl isolated RNA was spotted on a positively charged nylon membrane and cross-linked for 2 min under UV light. The probe to detect the 27S + 35.5 rRNA was labeled with digoxigenin using the PCR DIG Probe Synthesis kit (Roche) according to the manufacturer's instructions. The digoxigenin-labeled probe has a size of 232 bp and anneals with the 27S rRNA, the unprocessed variant of the 25S and 5.8S rRNA (corresponding to region of nucleotides 3,020–3,251 of the 35S rRNA). The membranes were hybridized over night at 50°C according to the protocol of the DIG Northern Blot Starter kit (Roche). Signals were detected with the antidigoxigenin antibody coupled to alkaline phosphatase (Roche) and the AP chemiluminescence substrate (Millipore) and visualized using the LAS 3000 (Fujifilm).

Downloaded from jcb.rupress.org on June 17, 2011

Published April 5, 2010

Purification and biotin labeling of ribosomes

For ribosome preparation, wt yeast cells were grown in 2 liters YPD to OD_{600} = 0.8 at 30°C and harvested. The cells were resuspended in CSB (300 mM sorbitol, 20 mM Hepes-KOH, pH 7.5, 1 mM EGTA, 5 mM $MgCl_2$, 10 mM KCl, 10% glycerol, and 2 mM β-mercaptoethanol) supplemented with 1 mM PMSF and protease inhibitor cocktail and lysed by French press. The lysate was cleared (30,000 *g* for 30 min) and layered on top of two volumes of a 20% (wt/vol) sucrose cushion in CSB without sorbitol containing 1 M KCl. The ribosomes were sedimented for 4 h at 200,000 *g*, resuspended in 4 ml CSB, and sucrose cushion centrifugation was repeated. The high salt–washed ribosomal pellet was resuspended in RB (20 mM Hepes-KOH, pH 7.5, 50 mM KCl, 6 mM $MgCl_2$, and 1 mM DTT).

For the biotinylation, 400 µl yeast ribosomes in RB were labeled with 5.8 µl NHS chromogenic biotin (EZ-Link; 12.33 µM in dimethylformamide; Thermo Fisher Scientific) for 70 min at room temperature. The excess of biotin was removed by gel filtration on a Zeba Desalt Spin column (2 ml; Thermo Fisher Scientific) equilibrated with RB, and labeled ribosomes were recovered by sedimentation for 50 min at 200,000 *g*. Ribosomes were resuspended in 400 µl RB, and aliquots were frozen in liquid N_2 prior to storage.

Analysis of association of biotin-labeled ribosomes with in vivo–formed aggregates

Yeast aggregates were prepared as described in Materials and methods. Cells from 150 ml logarithmic cultures were resuspended in 3 ml of lysis buffer (20 mM Na-phosphate, pH 6.8, 10 mM DTT, 1 mM EDTA, 0.1% Tween, 1 mM PMSF, protease inhibitor cocktail, 3 mg/ml zymolyase T20, and 1.25 U/ml DNase [Sigma-Aldrich]) and incubated at room temperature for 20 min. Upon sonication, the lysates were cleared, and the protein concentrations were adjusted in a volume of 2.4 ml using lysis buffer. 800 µl of each sample was used for direct preparation of aggregates (−R). The residual 1.6 ml of the lysates was mixed with 40 µl labeled yeast ribosomes, and 800 µl was used for aggregate preparation (+R*). The remaining 800 µl of the lysates (+R*/UC) was subjected to ultracentrifugation (50 min at 200,000 *g*). Pellets from aggregate preparations and ultracentrifugation were resolubilized in SDS sample buffer and applied to SDS-PAGE. Biotinylation was detected by Western blotting using StrepTactin-AP (IBA).

Online supplemental material

Fig. S1 shows the synthetic growth defect of cells deleted for zuotin and NAC, analysis of the heat shock response in cells lacking SSB and NAC, and phosphorylation of SNF1 in cells lacking SSB and NAC. Fig. S2 shows the dot blot analysis of RNA prepared from aggregates of chaperone-deficient cells and the analysis of biotin-labeled ribosomes, which do not cosediment with aggregates. Fig. S3 shows the ribosome profiles of Sse1-deficient cells. Table S1 lists details about yeast strains used in this study. Online supplemental material is available at http://www.jcb.org/cgi/content/full/jcb.200910074/DC1.

We thank the members of the Deuerling laboratory, R.D. Wegrzyn, K. Turgay, and M.P. Mayer for helpful discussions and comments to the manuscript. We particulary thank T. Riess and the INCIDE research center at the University of Konstanz for helping to evaluate ribosomal profiles. We are thankful to U. Dahl, J. Hentschel, and T. Ruppert for their expert technical assistance and M. Zimbelmann-Schardt for help in the polysome profiling.

This work was supported by a fellowship of the Boehringer Ingelheim Fonds to M. Erhardt, fellowships of the Konstanz Research School Chemical Biology to M. Koch, A. Scior, and S. Preissler, and grants of the Human Frontier in Science Program and of the DFG (DE-783) to E. Deuerling.

Submitted: 12 October 2009
Accepted: 9 March 2010

References

Albanèse, V., S. Reissmann, and J. Frydman. 2010. A ribosome-anchored chaperone network that facilitates eukaryotic ribosome biogenesis. *J. Cell. Biol.* 189:69–81.

Bailleul, P.A., G.P. Newnam, J.N. Steenbergen, and Y.O. Chernoff. 1999. Genetic study of interactions between the cytoskeletal assembly protein sla1 and prion-forming domain of the release factor Sup35 (eRF3) in *Saccharomyces cerevisiae*. *Genetics.* 153:81–94.

Basu, U., K. Si, J.R. Warner, and U. Maitra. 2001. The *Saccharomyces cerevisiae* TIF6 gene encoding translation initiation factor 6 is required for 60S ribosomal subunit biogenesis. *Mol. Cell. Biol.* 21:1453–1462. doi:10.1128/MCB.21.5.1453-1462.2001

Brachmann, C.B., A. Davies, G.J. Cost, E. Caputo, J. Li, P. Hieter, and J.D. Boeke. 1998. Designer deletion strains derived from *Saccharomyces cerevisiae* S288C: a useful set of strains and plasmids for PCR-mediated gene disruption and other applications. *Yeast.* 14:115–132. doi:10.1002/(SICI)1097-0061(19980130)14:2<115::AID-YEA204>3.0.CO;2-2

Bukau, B., E. Deuerling, C. Pfund, and E.A. Craig. 2000. Getting newly synthesized proteins into shape. *Cell.* 101:119–122. doi:10.1016/S0092-8674(00)80806-5

Chomczynski, P., and N. Sacchi. 1987. Single-step method of RNA isolation by acid guanidinium thiocyanate-phenol-chloroform extraction. *Anal. Biochem.* 162:156–159. doi:10.1016/0003-2697(87)90021-2

Demoinet, E., A. Jacquier, G. Lutfalla, and M. Fromont-Racine. 2007. The Hsp40 chaperone Jjj1 is required for the nucleo-cytoplasmic recycling of preribosomal factors in *Saccharomyces cerevisiae*. *RNA.* 13:1570–1581. doi:10.1261/rna.585007

Frydman, J. 2001. Folding of newly translated proteins in vivo: the role of molecular chaperones. *Annu. Rev. Biochem.* 70:603–647. doi:10.1146/annurev.biochem.70.1.603

Gautschi, M., A. Mun, S. Ross, and S. Rospert. 2002. A functional chaperone triad on the yeast ribosome. *Proc. Natl. Acad. Sci. USA.* 99:4209–4214. doi:10.1073/pnas.062048599

Goldstein, A.L., and J.H. McCusker. 1999. Three new dominant drug resistance cassettes for gene disruption in *Saccharomyces cerevisiae*. *Yeast.* 15:1541–1553. doi:10.1002/(SICI)1097-0061(199910)15:14<1541::AID-YEA476>3.0.CO;2-K

Güldener, U., G.J. Koehler, C. Haussmann, A. Bacher, J. Kricke, D. Becher, and J.H. Hegemann. 2004. Characterization of the *Saccharomyces cerevisiae* Fol1 protein: starvation for C1 carrier induces pseudohyphal growth. *Mol. Biol. Cell.* 15:3811–3828. doi:10.1091/mbc.E03-09-0680

Guthrie, C., and G.R. Fink. 2004. Guide to Yeast Genetics and Molecular Biology. Elsevier Academic Press, San Diego. 933 pp.

Hartl, F.U., and M. Hayer-Hartl. 2002. Molecular chaperones in the cytosol: from nascent chain to folded protein. *Science.* 295:1852–1858. doi:10.1126/science.1068408

Hundley, H., H. Eisenman, W. Walter, T. Evans, Y. Hotokezaka, M. Wiedmann, and E. Craig. 2002. The in vivo function of the ribosome-associated Hsp70, Ssz1, does not require its putative peptide-binding domain. *Proc. Natl. Acad. Sci. USA.* 99:4203–4208. doi:10.1073/pnas.062048399

Hundley, H.A., W. Walter, S. Bairstow, and E.A. Craig. 2005. Human Mpp11 J protein: ribosome-tethered molecular chaperones are ubiquitous. *Science.* 308:1032–1034. doi:10.1126/science.1109247

Hurt, E., S. Hannus, B. Schmelzl, D. Lau, D. Tollervey, and G. Simos. 1999. A novel in vivo assay reveals inhibition of ribosomal nuclear export in ran-cycle and nucleoporin mutants. *J. Cell Biol.* 144:389–401. doi:10.1083/jcb.144.3.389

Kim, S.Y., and E.A. Craig. 2005. Broad sensitivity of *Saccharomyces cerevisiae* lacking ribosome-associated chaperone ssb or zuo1 to cations, including aminoglycosides. *Eukaryot. Cell.* 4:82–89. doi:10.1128/EC.4.1.82-89.2005

Kramer, G., T. Rauch, W. Rist, S. Vorderwülbecke, H. Patzelt, A. Schulze-Specking, N. Ban, E. Deuerling, and B. Bukau. 2002. L23 protein functions as a chaperone docking site on the ribosome. *Nature.* 419:171–174. doi:10.1038/nature01047

Lacombe, T., J.J. García-Gómez, J. de la Cruz, D. Roser, E. Hurt, P. Linder, and D. Kressler. 2009. Linear ubiquitin fusion to Rps31 and its subsequent cleavage are required for the efficient production and functional integrity of 40S ribosomal subunits. *Mol. Microbiol.* 72:69–84. doi:10.1111/j.1365-2958.2009.06622.x

Lauring, B., H. Sakai, G. Kreibich, and M. Wiedmann. 1995. Nascent polypeptide-associated complex protein prevents mistargeting of nascent chains to the endoplasmic reticulum. *Proc. Natl. Acad. Sci. USA.* 92:5411–5415 doi:10.1073/pnas.92.12.5411

Longtine, M.S., A. McKenzie III, D.J. Demarini, N.G. Shah, A. Wach, A. Brachat, P. Philippsen, and J.R. Pringle. 1998. Additional modules for versatile and economical PCR-based gene deletion and modification in *Saccharomyces cerevisiae*. *Yeast.* 14:953–961. doi:10.1002/(SICI)1097-0061(199807)14:10<953::AID-YEA293>3.0.CO;2-U

Martinez-Hackert, E., and W.A. Hendrickson. 2009. Promiscuous substrate recognition in folding and assembly activities of the trigger factor chaperone. *Cell.* 138:923–934. doi:10.1016/j.cell.2009.07.044

Meyer, A.E., N.J. Hung, P. Yang, A.W. Johnson, and E.A. Craig. 2007. The specialized cytosolic J-protein, Jjj1, functions in 60S ribosomal subunit biogenesis. *Proc. Natl. Acad. Sci. USA.* 104:1558–1563. doi:10.1073/pnas.0610704104

Downloaded from jcb.rupress.org on June 17, 2011

Published April 5, 2010

Möller, I., B. Beatrix, G. Kreibich, H. Sakai, B. Lauring, and M. Wiedmann. 1998. Unregulated exposure of the ribosomal M-site caused by NAC depletion results in delivery of non-secretory polypeptides to the Sec61 complex. *FEBS Lett.* 441:1–5. doi:10.1016/S0014-5793(98)01440-9

Pfund, C., N. Lopez-Hoyo, T. Ziegelhoffer, B.A. Schilke, P. Lopez-Buesa, W.A. Walter, M. Wiedmann, and E.A. Craig. 1998. The molecular chaperone Ssb from *Saccharomyces cerevisiae* is a component of the ribosome-nascent chain complex. *EMBO J.* 17:3981–3989. doi:10.1093/emboj/17.14.3981

Pfund, C., P. Huang, N. Lopez-Hoyo, and E.A. Craig. 2001. Divergent functional properties of the ribosome-associated molecular chaperone Ssb compared with other Hsp70s. *Mol. Biol. Cell.* 12:3773–3782.

Powers, T., and P. Walter. 1996. The nascent polypeptide-associated complex modulates interactions between the signal recognition particle and the ribosome. *Curr. Biol.* 6:331–338. doi:10.1016/S0960-9822(02)00484-0

Raden, D., and R. Gilmore. 1998. Signal recognition particle-dependent targeting of ribosomes to the rough endoplasmic reticulum in the absence and presence of the nascent polypeptide-associated complex. *Mol. Biol. Cell.* 9:117–130.

Rauch, T., H.A. Hundley, C. Pfund, R.D. Wegrzyn, W. Walter, G. Kramer, S.Y. Kim, E.A. Craig, and E. Deuerling. 2005. Dissecting functional similarities of ribosome-associated chaperones from *Saccharomyces cerevisiae* and *Escherichia coli. Mol. Microbiol.* 57:357–365. doi:10.1111/j.1365-2958.2005.04690.x

Raue, U., S. Oellerer, and S. Rospert. 2007. Association of protein biogenesis factors at the yeast ribosomal tunnel exit is affected by the translational status and nascent polypeptide sequence. *J. Biol. Chem.* 282:7809–7816. doi:10.1074/jbc.M611436200

Reimann, B., J. Bradsher, J. Franke, E. Hartmann, M. Wiedmann, S. Prehn, and B. Wiedmann. 1999. Initial characterization of the nascent polypeptide-associated complex in yeast. *Yeast.* 15:397–407. doi:10.1002/(SICI)1097-0061(19990330)15:5<397::AID-YEA384>3.0.CO;2-U

Rospert, S., Y. Dubaquié, and M. Gautschi. 2002. Nascent-polypeptide-associated complex. *Cell. Mol. Life Sci.* 59:1632–1639. doi:10.1007/PL00012490

Sahi, C., and E.A. Craig. 2007. Network of general and specialty J protein chaperones of the yeast cytosol. *Proc. Natl. Acad. Sci. USA.* 104:7163–7168. doi:10.1073/pnas.0702357104

Sydorskyy, Y., D.J. Dilworth, E.C. Yi, D.R. Goodlett, R.W. Wozniak, and J.D. Aitchison. 2003. Intersection of the Kap123p-mediated nuclear import and ribosome export pathways. *Mol. Cell. Biol.* 23:2042–2054. doi:10.1128/MCB.23.6.2042-2054.2003

von Plehwe, U., U. Berndt, C. Conz, M. Chiabudini, E. Fitzke, A. Sickmann, A. Petersen, D. Pfeifer, and S. Rospert. 2009. The Hsp70 homolog Ssb is essential for glucose sensing via the SNF1 kinase network. *Genes Dev.* 23:2102–2115. doi:10.1101/gad.529409

Wang, S., H. Sakai, and M. Wiedmann. 1995. NAC covers ribosome-associated nascent chains thereby forming a protective environment for regions of nascent chains just emerging from the peptidyl transferase center. *J. Cell Biol.* 130:519–528. doi:10.1083/jcb.130.3.519

Wegrzyn, R.D., and E. Deuerling. 2005. Molecular guardians for newborn proteins: ribosome-associated chaperones and their role in protein folding. *Cell. Mol. Life Sci.* 62:2727–2738. doi:10.1007/s00018-005-5292-z

Wegrzyn, R.D., D. Hofmann, F. Merz, R. Nikolay, T. Rauch, C. Graf, and E. Deuerling. 2006. A conserved motif is prerequisite for the interaction of NAC with ribosomal protein L23 and nascent chains. *J. Biol. Chem.* 281:2847–2857. doi:10.1074/jbc.M511420200

Wiedmann, B., and S. Prehn. 1999. The nascent polypeptide-associated complex (NAC) of yeast functions in the targeting process of ribosomes to the ER membrane. *FEBS Lett.* 458:51–54. doi:10.1016/S0014-5793(99)01118-7

Wiedmann, B., H. Sakai, T.A. Davis, and M. Wiedmann. 1994. A protein complex required for signal-sequence-specific sorting and translocation. *Nature.* 370:434–440. doi:10.1038/370434a0

Downloaded from jcb.rupress.org on June 17, 2011